



haematologica

the hematology journal

19th Congress of
the European Hematology Association
Milan, Italy, June 12 - 15, 2014

ABSTRACT BOOK

2014 | s1

ISSN 0390-6078

Journal of the European Hematology Association
Published by the Ferrata-Storti Foundation, Pavia, Italy
Volume 99, supplement no. 1, June 2014
www.haematologica.org



set of alternative 5' exons; interestingly, this variant lacks the exon encoding for both the 5' untranslated region (5' UTR) as well as the intracellular and transmembrane domains of membrane-bound RANKL. Originally identified in two distinct squamous cell carcinoma cell lines, it has been suggested that variant 2 is predominantly expressed in malignant cell types. Recently, novel transcript variants of TNFSF11 were identified while it was shown that the longest open reading frame of variant 2 can be directly translated into the soluble form of RANKL, a protein linked causatively to induction of bone loss at distant sites in the skeleton. Importantly, translational dynamics of TNFSF11 variant 2 remain, yet, shadowy.

Aims: Provide, via bioinformatics analysis, novel insights on TNFSF11 variant 2 (soluble RANKL mRNA) translational dynamics; *id est* introduce this variant as a molecule of low translational efficiency. Highlight that a, yet unprecedented, shorter TNFSF11 variant could likely be translated into soluble RANKL in a more efficient manner.

Methods: Translational efficiency of TNFSF11 variant 2 was estimated with regard to the size of the 5' UTR, the tendency of this region for forming stable secondary structures and the number of pseudosignals; 5' UTR tendency for forming stable stem-loop structures was accessed via *pknotsRG-mfe* program. Soluble RANKL mRNA sequence was scanned for the presence of exonized Alus by *BLAST* and *Repeat Masker*. Search for uORFs was performed with the *ORF Finder* program; search parameters were set as previously suggested [Calvo *et al.*, 2009]. Alignment of corresponding sequences was schematically reproduced with the *Multalin* program.

Results: TNFSF11 variant 2 (Figure 1A, upper panel) represents a molecule of, likely, low translational efficiency, especially as compared to variant 1 (Figure 1B, 1C). Exons 1B and 1C of TNFSF11 variant 2 contain exonized Alus, of sense and antisense orientation, respectively (Figure 1A, upper panel). The exonized Alus potentially synergize in the formation of a complex stem-loop structure that could significantly impair translational efficiency, as indicated by the value for the secondary structures' minimum free energy (MFE) (Figure 1B, right panel). An evolutionary-induced single-nucleotide variation of the integrated AluSz element allows for the mutational gain of an upstream AUG trinucleotide (Figure 1A, green boxes) that demarcates the longest out of the five upstream open reading frames (uORFs) present in soluble RANKL mRNA. Both the start and stop codons of this uORF are conserved among higher primates (Figure 1A, lower panel) while, according to dbSNP, are not polymorphic in human. In addition, out of the 12 known polymorphic sites included within this uORF, all representing single nucleotide substitutions, none induces an in-frame nonsense codon; all the above could suggest an important biological role of this uORF, mainly in the context of post-transcriptional regulation. An alternative splicing event, exon 1C skipping, allows for the generation of a shorter TNFSF11 transcript variant (Figure 1D). Originally identified in the human osteoblast-like cell line Saos-2 and the human T cell line Jurkat Clone E6 [Walsh *et al.*, 2013], this variant contains also the primary ORF that encodes for the full length extracellular domain of RANKL (soluble RANKL). However exclusion of exon 1C results in, markedly, shortening the length and increasing the MFE of the 5' UTR while disrupts the uORF, described above.

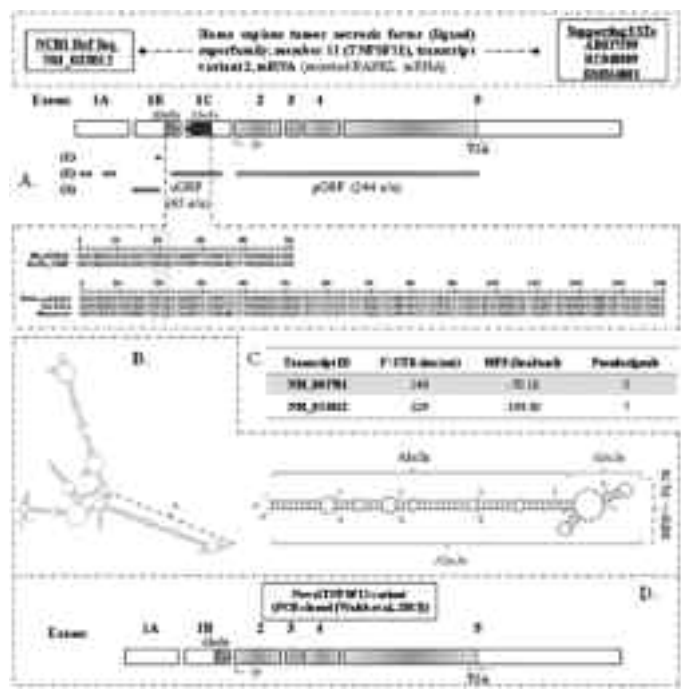


Figure 1.

Summary and Conclusion: Intriguingly, natural selection seems to have induced the assembly of stringent biological mechanisms that could significantly impair the translation of TNFSF11 variant 2. However a novel TNFSF11 variant, partially bypassing these constraints, could efficiently encode for soluble RANKL; *id est* this novel variant could be the one encoding for soluble RANKL, instead of TNFSF11 variant 2 as previously assumed.

P941

FIBROBLAST ACTIVATION PROTEIN PROTECTS BORTEZOMIB INDUCED APOPTOSIS IN MULTIPLE MYELOMA CELLS THROUGH B-CATENIN SIGNALING PATHWAY

Z Cai^{1,*}, J He¹, L Yang¹, X Han¹, G Zheng¹, W Zheng¹, G Wei¹, W Wu¹, X Ye¹, J Shi¹, W Xie¹, L Li¹, J Zhang¹, W Huang¹, H Huang¹, X Zhang², J Fu³

¹Hematology & Bone Marrow Transplantation, The First Affiliated Hospital of Medical School, Zhejiang University, ²Hematology, Hangzhou Red Cross Hospital, Hangzhou, ³Hematology, The People's Hospital of Shaoxing, Shaoxing, China

Background: Multiple myeloma(MM), a malignant plasma cells proliferative disease, is characterized by increased blood calcium level, renal insufficiency, anemia, and bone lesions(CRAB). The coevolution of MM cells with bone marrow stromal cells plays an important role in MM cells growth, survival and drug resistance. Fibroblast activation protein(FAP), a vital transmembrane protein which is expressed in 90% epithelial tumor stroma, has been reported to be involved in mediating drug resistance, tumor progression, immune evasion, invasion and metastasis of tumor cells. However, the expression and function of FAP in MM is still less known.

Methods: Bone marrow mesenchymal stem cells(BMMSCs) from MM patients, normal donors and the cell line of human BMMSCs were analyzed for expression of the FAP protein by semiquantitative real time-polymerase chain(qRT-PCR), flow cytometry(FCM) and immunofluorescence(IF). Tumor cell-conditioned medium (TCCM) from supernatant of MM cell lines were added to BMMSCs or MM cells coculture with BMMSCs to observe the effect of TCCM or MM cells stimulation for the expression of FAP. We further studied the function and mechanism of FAP in bortezomib induced apoptosis of myeloma cells by silencing FAP with small interfering RNA(siRNA). Apoptotic cells of MM cells were detected by APC-CD138/annexin V-FITC using flow cytometry analysis. Western blotting was used to elucidate the signaling pathway that FAP may be involved in mediating apoptosis of MM cells induced by bortezomib.

Results: There was no significant difference in the expression of FAP in hBMMSCs isolated from MM patients and normal donors(p<0.05) as determined by qRT-PCR, and FCM. BMMSCs stimulated by TCCM or coculture with MM cells displayed an elevated expression of FAP as detected by qRT-PCR(p<0.05). In the presence of 30nM bortezomib, MM cell lines RPMI8226 or CAG cells co-cultured with BMMSCs in which FAP was knockdown or not by siRNA for 48h demonstrated that FAP is capable of protecting RPMI8226 and CAG cells induced by bortezomib from apoptosis as determined by FCM(NC siRNA vs FAP siRNA, p<0.05). Further study showed that the activity of β-catenin was significantly elevated in RPMI8226 and CAG cells after co-cultured with BMMSC in the presence of bortezomib. Knockdown FAP can reduce the expression of β-catenin and its downstream target proteins, such as c-myc, survivin, cyclin D1 in RPMI8226 and CAG cells detected by western blot. The activation of β-catenin need MM-BMMSCs direct contact other than separated by transwell.

Summary and Conclusion: Taken together, our data indicated that the expression level of FAP was no difference between the BMMSCs isolated from MM patients and normal donors. The expression of FAP can be increased by TCCM stimulation or coculture with MM cells. Further study demonstrated that FAP can protect MM cells from apoptosis induced by bortezomib, which is likely through β-catenin signaling pathway. This protection need direct contact with BMMSCs.

P942

PRECLINICAL ANTIMYELOMA ACTIVITY OF THE ALKYLATING-HDACI FUSION MOLECULE EDO-S101 THROUGH DNA-DAMAGING AND HDACI EFFECTS

AA López-Iglesias^{1,*}, L San-Segundo¹, L González¹, S Hernández¹, D Primo², M Garayoa¹, T Paíno¹, A García-Gómez¹, T Mehrling³, MV Mateos¹, EM Ocio¹

¹Hematology, University Hospital of Salamanca and Cancer Institute Research (IBSAL), Salamanca, ²Vivia Biotech, Madrid, Spain, Madrid, Spain, ³Mundipharma, Berlin, Germany

Background: Alkylators such as melphalan are part of the backbone treatment of young and also elderly MM patients. Moreover, novel ones such as bendamustine have been used in several combinations with either proteasome inhibitors or IMiDs. EDO-S101 is a novel drug resulting from the fusion of a molecule of bendamustine with a vorinostat one, with the aim of increasing the efficacy of the alkylator through the HDACi-mediated chromatin relaxation that would make DNA more accessible to the damaging effect of bendamustine.

Aims: To study the efficacy and mechanism of action of EDO-S101 in human myeloma cell lines (HMCL) either alkylator sensitive and resistant, in freshly isolated MM patient cells and in a xenograft model of human MM.

Methods: Sensitivity to EDO-S101 was assessed by MTT in HMCLs and by flow cytometry in freshly isolated cells from 5 MM patients. *in vivo* efficacy was analyzed in a xenograft plasmocytoma model of MM1S in CB-17 SCID mice. For the evaluation of the mechanism of action several techniques were used to analyze apoptosis and changes in the cell cycle profile. Western blot and immunohistochemistry in tumors excised from treated mice were also employed. Calcsyn program was used to calculate synergy or additive effect with other anti-MM drugs.

Results: Among a panel of 6 HMCLs representative of MM heterogeneity, high sensitivity to EDO-S101 was observed in all of them independently of p53 status (IC50 values ranging from 1 to 5 µM). Furthermore EDO-S101 was also active in cells isolated from MM patients, with median IC50 of 5 µM (ranging from 1,8 to 8 µM) and, interestingly, EDO-S101 could overcome alkylators-resistance as it was active in melphalan resistant cells (U266-LR7 and RPMI8226-LR5). Regarding the *in vivo* efficacy, three weekly doses of EDO-S101 (60 mg/Kg iv) were able to significantly decrease tumor growth (time to reach 1.000 mm³ of 20 days for the control group as compared with 60 days for the treated mice) and also to prolong survival (p<0.05). Importantly, EDO-S101 was also active in mice bearing big tumors (3.000 mm³). With regards to toxicity, only some body weight loss was observed in the treated mice. Regarding the mechanism of action, EDO-S101 induced apoptosis *in vitro* as assessed by Annexin-V staining, loss of mitochondrial membrane potential and cleavage of caspases 8, 9, 7, 3 and PARP. Cell cycle profile showed an S and G2M arrest. Specifically, EDO-S101 induced apoptosis was dependent of a dual alkylating and HDACi mechanisms. As far as the alkylating mechanism is concerned, EDO-S101 induced double strand breaks (DSBs) as demonstrated by comet assay by immunofluorescence and by an increase in pH2AX by western blot, both *in vitro*, and *in vivo* by immunohistochemistry in tumors from treated mice. As a result, an activation of the DNA damage checkpoints was also demonstrated with clear increases in p53, p-CHK1 and p-CHK2. As mentioned, an HDACi effect could also be proven, as an increase in the acetylation of histones H3 and H4 were observed both *in vitro* and *in vivo*. Finally, among different combinations tested, EDO-S101, was synergistic when combined with bortezomib and with dexamethasone in double and also in triple combination (EDO-S101 + bortezomib + dexamethasone).

Summary and Conclusion: The *in vitro*, *ex vivo* and *in vivo* efficacy of EDO-S101 through an alkylator and a HDACi effect, provides the rationale for the investigations of this compound in clinical trials in MM. Probably a potential clinically relevant combination would be that including bortezomib + dexamethasone.

P943

SAR650984, A HUMANIZED ANTI-CD38 ANTIBODY, POTENTLY TARGETS CANCER CELLS THROUGH MULTIPLE MECHANISMS

T Cai^{1,*}, B Zhang¹, G Yang¹, Z Song¹, S Dai¹, T He¹, D Simard¹, S Licht¹, F Adrian¹, H Cheng¹, K Corzo¹

¹Sanofi, Cambridge, United States

Background: CD38 is a type II transmembrane glycoprotein with both ectozyme activity and receptor function that has been implicated in cancer cell adhesion, signal transduction and calcium signaling. CD38 is highly expressed at the surface of many hematological cancer cells. SAR650984 is a humanized IgG1 antibody targeting CD38 in early clinical development to treat patients with CD38⁺ hematological malignancies. Several mechanisms of action of SAR650984 have been identified including antibody-dependent cell-mediated cytotoxicity (ADCC), complement-dependent cytotoxicity (CDC), and direct cell death induction (ASH 2008 Abstract #2756). In addition, SAR650984 displays potent inhibition of recombinant CD38 ADP-ribosyl cyclase activity in a biochemical assay (AACR 2013, Abstract #4735).

Aims: To further characterize the mechanism of direct cell death induction and extracellular nucleotide modulation by SAR650984.

Results: The direct effects of SAR650984 on cancer cells were evaluated in a panel of multiple myeloma (MM) and diffuse large B-cell lymphoma (DLBCL) cells. In cancer cells with high CD38 expression levels, Annexin V positive staining increased significantly after SAR650984 treatment, which correlated with strong cell proliferation inhibition. Cell death induced by SAR650984 was further confirmed by detection of released cell death biomarker HMGB1 and Cyclophilin A in culture medium. SAR650984 induced cell death was independent of caspase activation and BCL2 family protein alterations but associated with homotypic cell adhesion, which was similar to the reported activity of anti-CD20 type II antibody GA101 (Blood, 117:4519, 2011). These findings reveal that unlike other anti-CD38 antibodies, SAR650984 is able to directly induce novel mode of cell death in the absence of cross-linker or immune cells which potentially will lead to improved tumor cell killing *in vivo*. To explore the impact of SAR650984 on CD38 ecto-enzymatic activities in cancer cells, we have developed a robust LC-MS-based cellular CD38 enzymatic assay that monitors the depletion of CD38 substrates nicotinamide adenosine dinucleotide (NAD) and the production of cyclic adenosine diphosphoribose

(cADPR) and adenosine diphosphoribose (ADPR) from CD38 cyclase and CD38 NAD glycohydrolase activities, respectively. Preliminary results demonstrate that in response to the treatment of SAR650984, CD38 cyclase activity in multiple myeloma and lymphoma cancer cells was significantly inhibited by more than 90% as shown by a rapid and dose-dependent decrease in the rate of both substrate NAD depletion as well as extracellular cADPR production. Interestingly, a significant reduction of intracellular cADPR (over 60%) was also observed after SAR650984 treatment. Emerging data suggest that nucleotides such as NAD and cADPR are important regulators of cell growth, survival and immune responses. The altered levels of nucleotides resulting from CD38 enzymatic inhibition by SAR65084 in tumor microenvironment therefore could contribute to the anti-tumor efficacy of the antibody. Additional studies to elucidate this activity are currently ongoing.

Summary and Conclusion: SAR650984 demonstrated unique properties of direct cell death induction and potent CD38 enzymatic inhibition on cancer cells in addition to its complement and immune cells mediated cytotoxicity. These results provide new insights toward understanding the multiple antitumor mechanisms of SAR650984.

P944

NETWORK OF MICRO RNA AND EPIGENETICS ARE ASSOCIATED WITH THE PROGRESSION OF MGUS AND MULTIPLE MYELOMA

H Handa^{1,*}, Y Masuda², H Hattori², A Kaneko², I Suda², L Alkebsi², T Saitoh², H Iriuchishima¹, M Takizawa¹, H Koiso³, A Isoda⁴, M Matsumoto⁴, M Sawamura⁴, KI Tahara¹, T Ishizaki¹, T Mitsui¹, H Shimizu¹, A Yokohama⁵, N Tsukamoto³, Y Nojima¹, H Murakami²

¹Department of Medicine and Clinical Science, ²Health Science, ³Oncology Center, Gunma University, Maebashi, ⁴Hematology, National Nishi-Gunma Hospital, Shibukawa, ⁵Blood Transfusion Service, Gunma University, Maebashi, Japan

Background: Micro RNAs (miRs) are small non-coding RNAs of 19-25 bases in length having ability to modulate gene expression and involved in carcinogenesis. Transcriptional silencing of tumor suppressor genes (TSG) in cancer cells is often associated with DNA methylation and histone deacetylation carried out by epigenetic modifiers DNMTs and HDACs. miRs can regulate DNMTs expression and promoters of several miRs are also hypermethylated suggesting network of miR and epigenetics in cancer cells.

Aims: To understand the interaction of miRs and epigenetics in multiple myeloma (MM) progression, we investigated correlation between miR and epigenetic modifiers expressions and promoter methylation of TSG and miRs in plasma cells in MM and MGUS.

Methods: Purified plasma cells of BM obtained from 71 of MM patients 29 of MGUS patients and 11 of control patients are subjected to the study after informed consent. This study was approved by IRB. MiRs and epigenetic modifiers' mRNA values were determined by real time PCR with Taqman probe or SYBR green and 2- $\Delta\Delta$ method. Methylation status of DNA were determined by methylation specific PCR (MSP).

Results: We found significant reduction of miRs 15a (mean values; 52.36, 85.95, 110.71; MM, MGUS and control respectively, p<0.001), 15b (55.05, 79.97, 103.86, p<0.001), 16a (55.53, 87.62, 101.14, p<0.001), 29a (55.91, 84.19, 97.14, p<0.001), 29b (58.14, 83.67, 103.00, p<0.001), 29c (10.91, 14.94, 59.50, p<0.001), 34a (103.11, 132.78, 1617.25, p<0.001), 34b (21.73, 71.43, 56.73, p<0.001), 34c (1771.02, 12816.17, 7830.79, p<0.001) along with elevation DNMT1, 3A and HDAC3, 5, 7, 9 in MM. DNMT1, 3A were elevated in MM than in MGUS and control subjects (p=0.03). DNMT3B expression was not different among subjects. In the MM cell lines, miR 29a and 29b expression were inversely correlated with DNMT1 mRNA expression (r=0.96, p=0.0003; r=0.86, p=0.014). In the patient samples, DNMT1 was inversely correlated with miR15a, miR15b, miR16, miR29a, miR29b (r=-0.435, p=0.003; r=-0.341, p=0.02, r=-0.332, p=0.03, r=-0.419, p=0.005, r=-0.407, p=0.006). DNMT3A was inversely correlated with miR15a, miR29a, miR29b, miR29c (r=-0.365, p=0.02; r=-0.315, p=0.04; r=-0.371, p=0.01; r=-0.315, p=0.04), DNMT3B was inversely correlated with miR15a, miR15b, miR29a, miR29b (r=-0.418, p=0.005; r=-0.385, p=0.01; r=-0.353, p=0.02; r=-0.358, p=0.02). HDAC3, 7, 9 expression were elevated in MM than in MGUS (p=0.03, p=0.001, p=0.001) and normal subjects (0.18, 1.1, 20.8) (p=0.01, p=0.017, p=0.012). HDAC1, 3, 7 were inversely correlated only with miR15a (r=-0.25, p=0.039, r=-0.27, p=0.025, r=-0.25, p=0.038). The sequential samples during the treatment showed opposite direction change between miRs and epigenetic modifiers, associating with refractoriness. The rate of methylation in TSG was higher in MM and interestingly putative tumor suppressor miR 34a, b/c were also methylated. There were significant positive correlations among miRs expressions; miR29a-29b r=0.832, 29a-29c r=0.616, 29a-34a r=0.448, p<0.001, 29a-34b r=0.309, p=0.001, miR29a-miR34c r=0.414, p<0.001, miR29b-29c r=0.659, 29b-34a r=0.500, p<0.001, 29b-34b r=0.297, p=0.002, 29b-34c r=0.392, p<0.001, 29c-34a r=0.432, 29c-34b r=0.396, r=0.655, 29c-34c r=0.398, p<0.001. Covariance structure analysis revealed the complex network between miRs and epigenetics. When the cell lines were treated with 5 deoxy-azacytidine, miR34a, b, c expression levels increased after the treatment.

Summary and Conclusion: We found significant reduction of miRs expression